10Gb/s GaAs PHEMT Current Mode Transimpedance Preamplifier for Optical Receiver*

Jiao Shilong[1,2,†], Ye Yutang[1], Chen Tangsheng[2], Feng Ou[3], Jiang Youquan[3], Fan Chao[1], and Li Fuxiao[3]

(1 *School of Optoelectronic Information, University of Electronic Science and Technology of China, Chengdu* 610054, *China*)
(2 *National Key Laboratory of Monolithic Integrated Circuits and Modules, Nanjing* 210016, *China*)
(3 *Nanjing Electronic Devices Institute, Nanjing* 210016, *China*)

Abstract: A single power supply common-gate (CG) current mode transimpedance preamplifier (TIA) is developed with a 0.5μm GaAs PHEMT process. The amplifier has a measured −3dB bandwidth of 7.5GHz and a transimpedance gain of 45dBΩ. Both the input and output voltage standing wave ratios (VSWR) are less than 2 within the bandwidth. The equivalent input noise current spectral density varies from 14.3 to 22pA/$\sqrt{\text{Hz}}$, with an average value of 17.2pA/$\sqrt{\text{Hz}}$. Having a timing jitter of 14ps and eye amplitude of about 138mV, the measured output eye diagram for 10Gb/s NRZ pseudorandom binary sequence (PRBS) is clear and satisfactory.

Key words: GaAs PHEMT; current mode; preamplifier; noise figure; eye diagram
EEACC: 1220
CLC number: TN722.3 **Document code**: A **Article ID**: 0253-4177(2007)01-0024-07

1 Introduction

Preamplifiers are key components in long haul optical fiber communication systems. They take the very weak photocurrent from a photodetector and output the preliminary amplified signal in the form of voltage for further amplification. Thus a high transimpedance gain with large bandwidth and low equivalent input noise current spectral density for a preamplifier are desirable. Unfortunately, these requirements are conflicting in general, and tradeoffs must be made. In lumped parameter design, the transimpedance topology tunes the gain, bandwidth, and noise figure easily by only the selection of a feedback resistor. This seems to be the most common solution to the problem.

Depending on the electrical parameter dealt by the circuits, a transimpedance preamplifier can be classified as either a voltage mode amplifier or a current mode amplifier. As compared with the former using a common-source (CS)/common-emitter input stage, the current mode transimpedance amplifier takes advantage of the low input impedance of a common-gate/common-base transistor to reduce the input node associated pole time constant, relaxing the selection of capacitive photodetectors and broadening the bandwidth effectively[1]. Moreover, a higher transimpedance gain and a lower equivalent input noise current spectral density have also been reported in current mode transimpedance design[2]. Thus it is a very competitive choice for an optical receiver preamplifier.

However, the current mode TIA inherently suffers from relatively poor noise due to the fact that the load noise contributions of the common-gate input stage are directly referred to the input, so very large bias resistances of the CG stage, as well as large transconductance of the CG and CS transistors, are selected for low noise, and two power supplies are required for biases[2,3]. In our work, a single power supply scheme, with the benefits of low power dissipation and convenience of use, is developed for a 10Gb/s moderate noise cur-

* Project supported by the National Natural Science Foundation of China (No.60277008) and the National Key Laboratory of Monolithic Integrated Circuits and Modules Foundation of China (No.51491050105DZ0201)
† Corresponding author. Email: j_shilong@163.com
Received 7 August 2006, revised manuscript received 27 August 2006

rent density common-gate current mode TIA. Below, the design considerations are discussed in detail, and the simulated and measured results are also presented.

2　Circuit design

2.1　PHEMT device

We designed the circuit using 0.5μm gate length low noise GaAs PHEMTs of Nanjing Electronic Devices Institute, which has a characteristic frequency f_T of 30GHz. The cross-section and *I-V* curves of the PHEMT are shown in Figs. 1 (a) and (b), respectively.

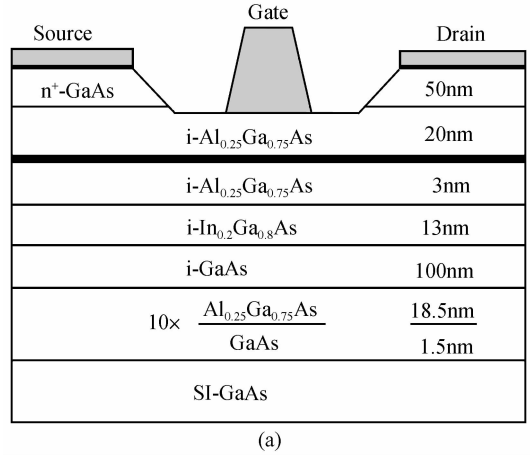

Fig. 1　(a) Cross-section of GaAs PHEMT; (b) Measured *I-V* curves

2.2　Fundamental principles

A schematic of the current mode transimpedance amplifier, constructed by a common-gate input stage, a common-source gain stage, and two source followers, is shown in Fig. 2. When a current signal from the photodetector is fed to the source terminal of P1, it travels to the drain with unit gain and is absorbed into the common-source stage. It then takes the form of a voltage at the gate of P2 and is amplified by the transconductance. Then the current signal at the drain of P2 is transformed into voltage again by the loads. After passing through the two voltage buffers of P3 and P5, the amplified signal reaches the out port.

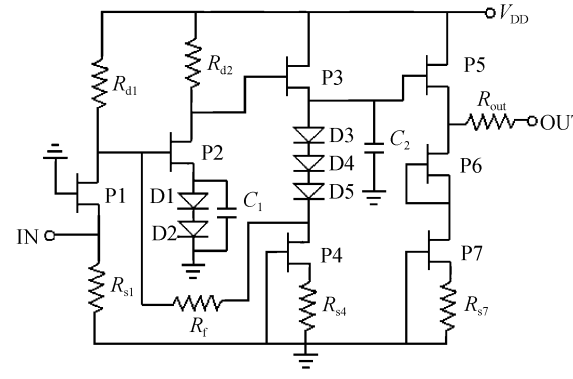

Fig. 2　Schematic of current mode TIA

In this schematic, the components R_{d1} and R_{s1} act as the bias resistances of P1, while R_{d1} also has a close relation with the total noise current. R_{d2} is the load of P2, playing an important role in open-loop gain and transmission delay. The Schottky diodes D1～D5, fabricated by drain-source direct connection of the PHEMT, elevate the source levels of P2 and P3 to provide proper negative bias, and the shunt capacitance C_1 tends to reduce the negative feedback caused by D1 and D2 to improve the small signal gain, especially at high frequencies. A feedback resistance R_f is applied from the source of P3 to the gate of P2, through which a shunt-shunt negative feedback is formed. To improve the gain shape and broaden the bandwidth, a peaking capacitance C_2 is placed between the two source followers. By the selection of R_{s4} and R_{s7}, the output of the two current sources P4 and P7 can be tuned, which is very important for P3 and P5 to get proper biases in this single power supply scheme. Finally, the second source follower P5 must be selected deliberately, or else an extra resistance R_{out} must be placed in order to get a good output standing wave ratio.

2.3　Gain and bandwidth

When the preamplifier is connected to a pho-

todetector, which has output impedance in the form of $R + 1/j\omega C$, where R is the series resistance and C is the junction capacitance, it is very important to realize a good match between the amplifier and photodetector to yield the largest gain and smallest ripples. The input impedance of the common-gate PHEMT is about $1/g_m$, which is dependent on the biases, as shown in Fig. 3 (a), where the drain voltage V_{d1} of P1 is 2V and V_{s1} varies from 0 to 1V in steps of 0.05V. From the Smith chart, we can select an operating point for matching in terms of the output impedance of the photodetector, and the smallest input impedances of the common-gate PHEMT and the photodetector can also be selected to minimize the input node associated pole time constant for an optimal bandwidth. However, because the current gain will decrease markedly with the frequency when V_{gs1} approaches the pinch-off voltage, as shown in Fig. 3 (b), these operating points should be avoided.

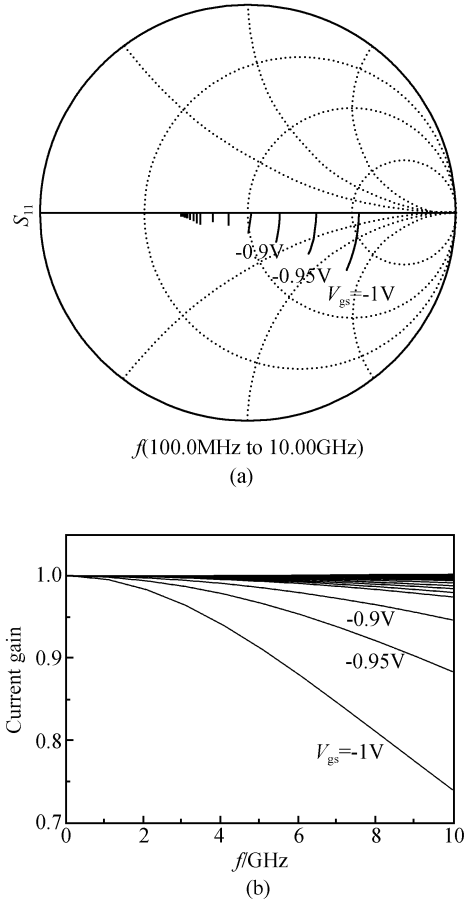

Fig. 3 Operating point selection of common-gate PHEMT (a) Reflection coefficient; (b) Current gain

The current mode TIA shown in Fig. 2 can also be divided into two parts: one is the common-gate input stage; the other is a conventional common-source TIA. Because the unit current gain of the CG stage and R_{d1} is set to be much larger than the input impedance of the CS amplifier, the input signal current at the source of P1 equals the input of the CS amplifier approximately. Therefore, with the single dominant pole assumption and without the influence of peaking capacitance C_2 for simplicity, the transimpedance gain of a current mode TIA will be the same as that of a CS TIA, and can be expressed as follows[4]:

$$Z_T \cong \frac{-R_f}{1 + j2\pi f R_f\left(C_{gd2} + \frac{C_{gs2}}{A} + \frac{1}{j2\pi f R_f A}\right)} \quad (1)$$

Taking the photodetector into account, the -3dB bandwidth of the current mode TIA is[5]

$$f_{-3dB} \cong \frac{1 + A}{2\pi R_f(C_{gd1} + C_{gs2} + (1 + A)C_{gd2})} \quad (2)$$

and the -3dB bandwidth of a conventional CS TIA is

$$f'_{-3dB} \cong \frac{1 + A}{2\pi R_f(C_{PD} + C_{gs2} + (1 + A)C_{gd2})} \quad (3)$$

where $A = g_{m2}R_{d2}$ is the open-loop DC gain, and C_{PD} is the output capacitance of photodetector and varies from several tens to hundreds of femtofarads.

From Eqs. (1) and (2), we can see that the transimpedance gain and -3dB bandwidth will improve with the increase of the open-loop gain A, but there are two limits: (1) The bandwidth is degraded by the Miller effect, especially in the case of a large open-loop gain; (2) The increase of open-loop gain will cause more propagation delay and phase shift, but the stability and a relatively better pulse response waveform should be ensured by a certain phase margin (PM), especially at high bit rates.

The bandwidth advantage of a current mode TIA can be found by a comparison of Eqs. (2) and (3). The photodetector output capacitance C_{PD}, which is one of the main adverse factors to bandwidth in CS TIAs, as shown in Eq. (3), is effectively isolated from the determination of bandwidth in current mode TIAs. That is, by the introduction of a common-gate input stage, the dominant pole depends on the gate-drain capacitance (C_{gd1}) of P1, the input capacitance of P2 and the feedback resistance, rather than the photodetector

output capacitance C_{PD}, the input capacitance of P2 and the feedback resistance as before. Because C_{gd1} (several tens of femtofarads at most) is smaller than C_{PD} in general, the current mode TIA can thus yield a larger bandwidth. Moreover, with the same bandwidth, the feedback resistance in a current mode TIA can be enlarged for a higher gain and a lower noise current, as shown below.

2.4 Noise analysis

Perhaps a major disadvantage of common-gate topologies is the direct relation of load noise current to the input. This effect arises from the unit current gain of such circuits, a point of contrast to common-source amplifiers[6]. The equivalent input noise current spectral density of the current mode TIA in Fig. 2 is given by[2]

$$S_{eq}(f) = \frac{4kT}{R_f} + \frac{4kT}{R_{d1}} + 2qI_{g1} + 2qI_{g2} + \frac{4kT\Gamma}{g_{m1}} \times \left[\frac{1}{R_{d1}^2} + \frac{1}{R_f^2} + (2\pi f)^2 (C_{PD} + C_{gs1})^2\right] + \frac{4kT\Gamma}{g_{m2}} \times \left[\frac{1}{R_{d1}^2} + \frac{1}{R_f^2} + (2\pi f)^2 (C_{gd1} + C_{gd2} + C_{gs2})^2\right] \quad (4)$$

where Γ is the noise factor.

The first two terms show the thermal noise given by R_f and R_{d1}, respectively. The next two terms represent the noise contributions due to gate leakage currents, which can be assumed to be negligible. The last two terms are the channel thermal noise of PHEMTs. According to Eq. (4), R_f and R_{d1} should be made as large as possible, unlike C_{PD}, to reduce their noise contributions, while the other parameters C_{gs1}, C_{gs2}, C_{gd1}, C_{gd2}, g_{m1}, g_{m2}, and Γ, depending on PHEMT material, physical dimension and bias, should be optimized for low noise. For example, a larger transconductance g_{m1} of P1 is desirable, but C_{gs1} and C_{gd1} will inevitably increase at the same time due to a larger gate width, or the bias voltage of P1, determined by R_{d1}, R_{s1}, and R_f in our single power supply scheme, should be tuned, but this often leads to a conflict with the minimizing of the noise current caused by these resistances. Furthermore, the drain voltage variation of P1 also affects the gate-source bias of the common-source gain stage. As a result, the transconductance of g_{m2} will change, and so will the open-loop gain and the total noise current. When it comes to a large g_{m2} for a low noise current, according to Eq. (4), similar things will happen to R_{d1}, R_{s1}, R_f, R_{d2}, C_{gs2}, C_{gd2}, and g_{m1}, as well as the transimpedance gain Z_T and bandwidth f_{-3dB}.

By now, one can see that some parameters act on each other and there are many tradeoffs among transimpedance gain, bandwidth, and noise. Compared with the works in Refs. [2, 3], where two power supplies were applied in the designs of current mode TIAs, more attention should be paid here to the optimal performance.

2.5 Capacitive peaking

Peaking technology is often used to broaden the bandwidth of a preamplifier in optical receiver designs[7,8]. Unlike inductive peaking, where inductors are placed in strategic locations in the circuits to resonate with parasitic capacitances to broaden the bandwidth, capacitive peaking adds an extra pole to the transfer function, resulting in the cancellation of the imaginary part in the denominator for improved bandwidth[7]. Since the size of a capacitor is smaller than that of an inductor, the parasitic effect, which may cause a bandwidth degradation rather than an improvement[8], can effectively be reduced in capacitive peaking. In our design, a capacitance C_2 is placed between the two source followers, as shown in Fig. 2, through which the small signal gain shape and bandwidth can easily be tuned, as shown in Fig. 4(a).

It is very useful for the gain shape and bandwidth to be tuned when process variation or device model deviation occurs in MMIC fabrication. However, the capacitance should also be selected prudently because the peaking effect can cause extra propagation delay and phase shift, potentially leading to a stability problem, and an overshoot of gain shape of no more than 10% may be accepted in many applications[9].

The decrease of phase margin due to the peaking effect may cause ringing in the time response. PM = 60° is typically considered to be the optimum value for achieving fast settling with little ringing[6]. In Fig. 4 (a), the capacitance values of 0, 0.08, and 0.2pF correspond to the phase margins of 62.2°, 58.7°, and 51.6°, respectively. The output eye diagram of the TIA, being a convenient way to evaluate the performance of a digital optical receiver, is also shown in Figs. 4 (b)

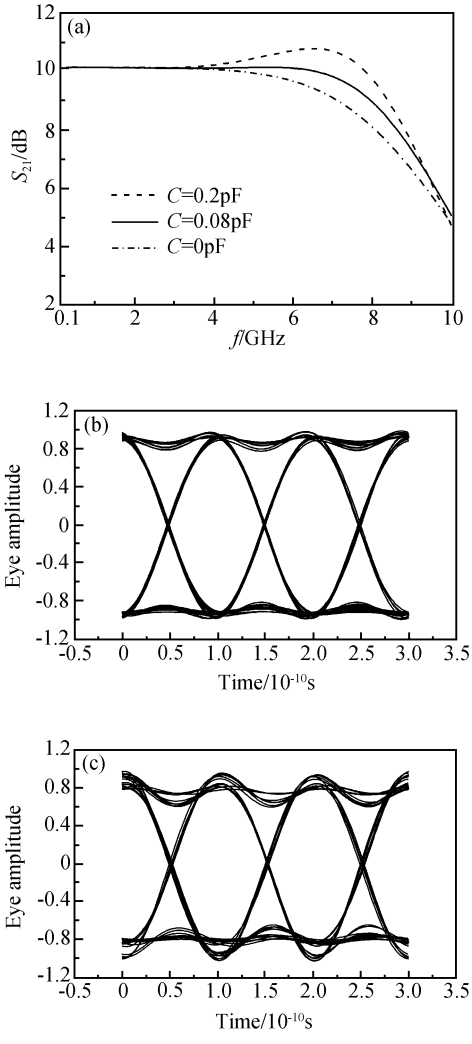

Fig. 4 (a) Gain and bandwidth improvement with capacitive peaking; (b) 10Gb/s output eye diagram with C_2 = 0pF; (c) 10Gb/s output eye diagram with C_2 = 0.2pF

and (c), where the amplitude is normalized and the influence of capacitive peaking is obvious.

2.6 Stability

After the schematic simulation, in which the resistances, capacitances and microstrip lines are treated as ideal components, the circuit should be simulated with ADS momentum software to ensure that the performance, especially the stability at high frequencies, is not degraded by layout and parasitic parameters. The momentum simulation results are shown in Fig. 5, from which we can see that the stable factor $K>1$ and $|\Delta| = |S_{11}S_{22} - S_{12}S_{21}|<1$ in the range of 100kHz~10GHz. Thus our design satisfies the absolute stability criterion.

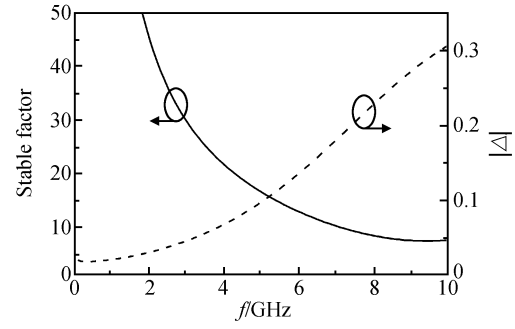

Fig. 5 Simulated stability criterion

3 Circuit performance

The fabricated die, with an area of 850μm × 1050μm, is shown in Fig. 6 (a). The die and off-die components, such as blocking and grounding capacitors or chocking inductor, would be assembled into a special package before measurement, as shown in Fig. 6 (b). The TIA, biased through the needles on both sides of the package, is connected with 50Ω microstrip lines, and two SMA connectors for signal input and output terminate the ends. The operating voltage is 5V with a total DC current of 60mA.

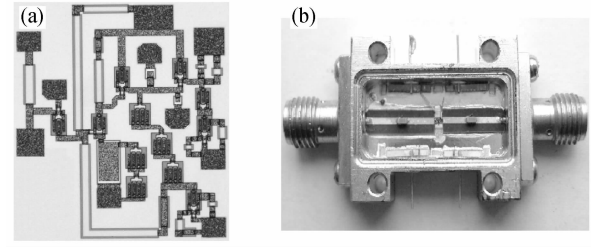

Fig. 6 (a) Photograph of die; (b) Assembly of TIA for measurement

We measured the S parameter under −30dBm input power, using an Agilent 8720ES vector network analyzer (VNA), and the results are shown in Fig. 7. The TIA has a flat forward gain curve of S_{21} around 10dB from 50MHz, which is the low frequency limit of the VNA, to about 6GHz, while the −3dB bandwidth is 7.5GHz. The input and output VSWR are less than 2 within the bandwidth. Considering the very low reverse gain of S_{12} ($\leqslant$ −32dB), the relation between the S parameter and transimpedance gain Z is[10]

$$Z_T(\Omega) = \frac{Z_0 S_{21}}{1 - S_{11}} \tag{5}$$

where Z_0 = 50Ω is the system impedance, and the

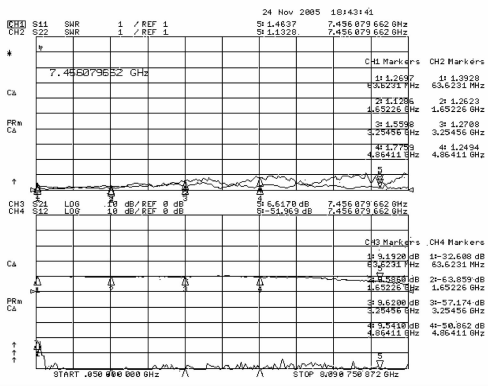

Fig. 7　Measured small signal S parameter

transimpedance gain is about 45dBΩ.

The noise figure (NF), measured by an Agilent N8975A noise figure analyzer, varies in the range of 4.16～7.8dB from 0.25 to 7.5GHz, with an average value of 5.5dB. The relation between equivalent input noise current and noise figure can approximately be expressed as[11,12]

$$\overline{i_{\mathrm{eq}}^2} = \frac{4kTB(10^{\mathrm{NF}/20} - 1)}{Z_0} \tag{6}$$

where B is the bandwidth. The simulated (smooth line) and measured (dotted line) curves of equivalent input noise current spectral density, based on Eq.(4) and the measured noise figure, respectively, are shown in Fig. 8. The two curves have a good coincidence in variation tendency, except the differences of 2.3～4pA/$\sqrt{\mathrm{Hz}}$, which are probably due to the process variation of resistances and the operating point deviations of PHEMTs.

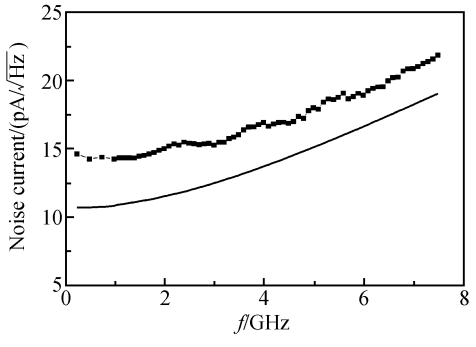

Fig. 8　Simulated (smooth line) and measured (dotted line) equivalent input noise current spectral density

As a preamplifier, the TIA should have a large linear range for some applications. We measured the output $P_{1\mathrm{dB}}$ at the frequency of 5GHz, using an Agilent E4419B power meter and an E8251A signal generator. From Fig. 9, we can see that the output $P_{1\mathrm{dB}}$ is about 1.8dBm, corresponding to a peak-to-peak current of 15.6mA in a 50Ω system. In view of the small signal gain of S_{21}, the linearity can meet the needs in many cases.

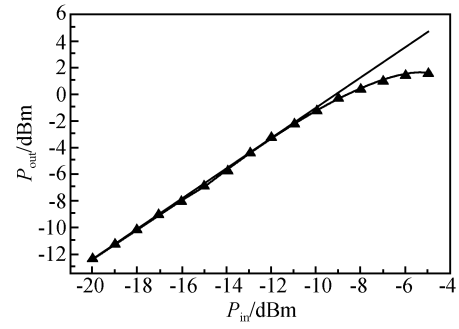

Fig. 9　Output $P_{1\mathrm{dB}}$ measurement

In order to evaluate the time domain performance of the TIA, we measured the eye diagram for 10Gb/s NRZ pseudorandom binary sequence (PRBS), using ADVANTEST D3186 pulse pattern generator and an Agilent 86100A oscilloscope. The output eye diagram, having a timing jitter of 14ps and $V_{\mathrm{p\text{-}p}}$ of about 138mV, is shown in Fig. 10 (b). However, because there is a long time delay at the end of the rising/falling edges in the input signal eye diagram, shown in Fig. 10 (a), the output eye diagram in Fig. 10 (b) seems somewhat asymmetric. That is, the output eye diagram will be improved further once the input signal distortion is eliminated.

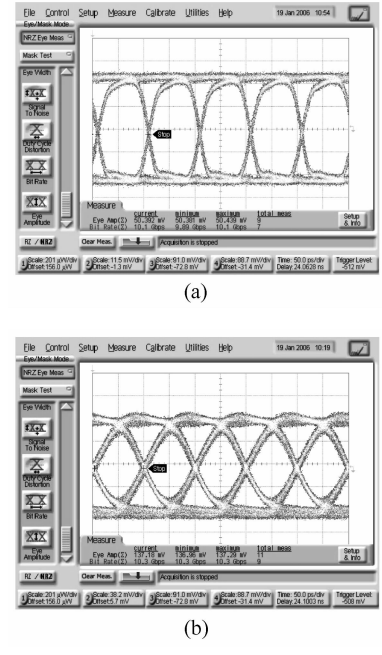

(a)

(b)

Fig. 10　Eye diagram measurement for 10Gb/s NRZ pseudorandom binary sequence　(a) Eye diagram of input signal; (b) Eye diagram of output signal

4 Conclusions

We have developed a single power supply current mode transimpedance preamplifier, using a 0.5μm low noise GaAs PHEMT MMIC process of Nanjing Electronic Devices Institute. The interactions of the electrical parameter and the tradeoffs among the gain, bandwidth and noise are discussed in detail. The TIA has a flat small signal gain curve and a moderate equivalent input noise current spectral density. Considering the input signal distortion, the measured output eye diagram for a 10Gb/s NRZ pseudorandom binary sequence is satisfactory.

Acknowledgements The author would like to thank the relevant personnel of the GaAs Engineering Center of Nanjing Electronic Devices Institute for the fabrication and measurement of the chip, Wang Zhigong and Li Wei of Institute of RF & OE-IC of the Southeast University for their help in the eye diagram measurement.

References

[1] Wilson B, Darwazch I. Transimpedance optical preamplifier with a very low input resistance. Electron Lett, 1987, 23: 88

[2] Toumazou C, Park S M. Wideband low noise CMOS transimpedance amplifier for gigaherz operation. Electron Lett, 1996, 32(13): 1194

[3] Vanisri T, Toumazou C. Low-noise optimization of current-mode transimpedance optical preamplifier. Proc IEEE ISCSA, 1993: 966

[4] Miyashita M, Maemura K, Yamamoto K, et al. An ultra broadband GaAs MESFET preamplifier IC for a 10 Gb/s optical communication system. IEEE Trans Microw Theory Tech, 1992, 40(12): 2439

[5] Laker K R, Sansen W M C. Design of analog integrated circuits and systems. McGraw-Hill, 1994

[6] Razavi B. Design of analog CMOS integrated circuits. McGraw-Hill, 2001

[7] Chien F T, Chan Y J. Bandwidth enhancement of transimpedance amplifier by a capacitive-peaking design. IEEE J Solid-State Circuits, 1999, 34(8): 1167

[8] Ohkawa N. Fiber-optic multigigabit GaAs MIC front-end circuit with inductor peaking. J Lightwave Technol, 1988, 6(11): 1665

[9] Abraham M. Design of butterworth-type transimpedance and bootstrap-transimpedance pre-amplifiers for fiber-optic receivers. IEEE Trans Circuits Syst, 1982, CAS-29(6): 375

[10] Laursen K, Yuan C, Chu D. Design high-speed MMICs and OEICs for 10Gb/s and 40Gb/s optical transponder front-ends. IEEE GaAs Digest, 2002: 221

[11] Park M S, Minasian R A. Ultra-low-noise and wideband-tuned optical receiver synthesis and design. J Lightwave Technol, 1994, 12(2): 254

[12] Goyal R. Monolithic microwave integrated circuits: technology and design. New York: Artech House, 1989

10Gb/s GaAs PHEMT 电流模跨阻抗光接收机前置放大器*

焦世龙[1,2,†] 叶玉堂[1] 陈堂胜[2] 冯 欧[3] 蒋幼泉[3] 范 超[1] 李拂晓[3]

(1 电子科技大学光电信息学院，成都 610054)
(2 单片集成电路与模块国家级重点实验室，南京 210016)
(3 南京电子器件研究所，南京 210016)

摘要： 采用 0.5μm GaAs PHEMT 工艺研制了一种单电源共栅电流模跨阻抗前置放大器(TIA). 测量得到放大器 −3dB 带宽为 7.5GHz，跨阻增益为 45dBΩ；输入输出电压驻波比(VSWR)均小于 2；等效输入噪声电流谱密度在 14.3～22pA/$\sqrt{\text{Hz}}$之间，平均值为 17.2pA/$\sqrt{\text{Hz}}$. 在输入 10Gb/s 非归零(NRZ)伪随机二进制序列(PRBS)信号下，放大器输出眼图清晰，具有 14ps 的定时抖动和 138mV 的峰峰电压.

关键词： GaAs PHEMT；电流模式；前置放大器；噪声系数；眼图
EEACC： 1220
中图分类号： TN722.3 **文献标识码：** A **文章编号：** 0253-4177(2007)01-0024-07

* 国家自然科学基金(批准号：60277008)和单片集成电路与模块国家级重点实验室基金(批准号：51491050105DZ0201)资助项目
† 通信作者. Email: j_shilong@163.com
2006-08-07 收到，2006-08-27 定稿